Integrated framework for assessing climate change impact on extreme rainfall and the urban drainage system

Wei Lu and Xiaosheng Qin IWA

ABSTRACT

Urban areas are becoming increasingly vulnerable to extreme storms and flash floods, which could be more damaging under climate change. This study presented an integrated framework for assessing climate change impact on extreme rainfall and urban drainage systems by incorporating a number of statistical and modelling techniques. Starting from synthetic future climate data generated by the stochastic weather generator, the simple scaling method and the Huff rainfall design were adopted for rainfall disaggregation and rainfall design. After having obtained 3-min level designed rainfall information, the urban hydrological model (i.e., Storm Water Management Model) was used to carry out the runoff analysis. A case study in a tropical city was used to demonstrate the proposed framework. Particularly, the impact of selecting different general circulation models and Huff distributions on future 1-h extreme rainfall and the performance of the urban drainage system were investigated. It was revealed that the proposed framework is flexible and easy to implement in generating temporally high-resolution rainfall data under climate model projections and offers a parsimonious way of assessing urban flood risks considering the uncertainty arising from climate change model projections, downscaling and rainfall design.

Key words | climate change, extreme rainfall, simple scaling, temporal disaggregation, urban drainage

Wei Lu
Xiaosheng Qin IWA (corresponding author)
School of Civil and Environmental Engineering,
Nanyang Technological University,
50 Nanyang Avenue,
Singapore 639798
E-mail: xsqin@ntu.edu.sg

INTRODUCTION

Climate change impact is projected to pose a profound effect on many aspects of water resource systems, and the number and severity of extreme storms are expected to increase over many urban areas around the world (IPCC 2007; Olsson et al. 2009; Fischer & Knutti 2016; Lu et al. 2019). As such extreme events would elevate the risk of flash flood problems, it is imperative to address the climate change effect when the improvement of current drainage systems or the design of new systems are needed for long-term usage. Over the past decades, a large number of research works have been reported to assess climate change impacts on urban rainfall extremes and drainage systems (Willems et al. 2012; Langeveld et al. 2013; Lu & Qin 2014; Bi et al. 2017). Most of these studies relied on combinative efforts of general circulation model (GCM) projection, downscaling and hydrological modelling (Sharma et al. 2007; Semadeni-Davies et al. 2008a, 2008b; Shrestha 2013; Herath et al. 2016; Alamdari et al. 2017).

Specifically, Willems (2013) statistically analysed and downscaled a large ensemble of GCMs and local regional climate models (RCMs) in Belgium. After deriving changes in intensity–duration–frequency (IDF) curves, the study established a conceptual reservoir model to quantify the discharge rate under future extreme scenarios and found that up to 50% increase in the storage capacity would be needed to keep the future overflow frequency at the current

level. Le *et al.* (2014) assessed the impact of climate change on the urban drainage flow through automated statistical downscaling and *K*-nearest neighbour-based disaggregation. Shrestha *et al.* (2014) assessed the impact of climate change on the urban drainage flow by comparing two approaches for generating future climatic scenarios. The first one adopted dynamic downscaling which linked the GCM with the RCM, and the second one followed hypothetical increments of baseline rainfall conditions by percentages. Zahmatkesh *et al.* (2015) studied the climate change effect on urban runoff in a river watershed where downscaling and disaggregation methods were used to obtain hourly rainfall time series. Neumann *et al.* (2015) employed three GCMs to project future climate scenarios and established a simplified model to address the excessive runoff volume and adaptation costs for urban drainage systems in 19 cities of the USA.

More recently, Shrestha *et al.* (2017) proposed a spatial downscaling and temporal disaggregation method for developing future IDF curves using the Long Ashton Research Station Weather Generator (LARS-WG) (Semenov *et al.* 2002; Semenov & Stratonovitch 2015) and the rainfall disaggregation tool, HYETOS (Koutsoyiannis & Onof 2001). A correction factor for bias elimination was adopted to mitigate the underestimation problem encountered in calibrating the modelled data by using observed IDF curves. Kristvik *et al.* (2018) applied an integrated spatial–temporal downscaling method, which combined Statistical DownScaling Model – Decision Centric (SDSM-DC) and the Generalized Extreme Value (GEV) distribution to project future rainfall and generate IDF curves in the city of Bergen. The study also investigated the effect of rain gardens as an adaptation measure to climate change.

From the previous works, it is revealed that statistical downscaling and disaggregation methods are commonly used to generate climate variables (mainly rainfall) for urban hydrological studies. However, due to the fine-resolution requirement of climate data both temporally and spatially at an urban scale (even at the minutes level), it is still a challenging task to carry out the climate change impact study for urban drainage systems using individual statistical or modelling methods. Although very limited attempts were made using holistic approaches involving downscaling, disaggregation, rainfall design and hydrological simulation (e.g., Shrestha *et al.* 2017), the connection of various modules

was rather complex, and there were still issues with bias correction, uncertainty consideration and model validation. In addition, there are few previous works focused on tropical regions, which are normally characterized by monsoons and intense rainfall with short durations (Fong 2012). It is desired that a more straightforward and flexible approach be proposed for the mentioned purpose.

Therefore, the objective of this study is to propose an integrated framework for assessing climate change impact on extreme rainfall and urban drainage systems. The framework follows a top-down strategy, covering downscaling and disaggregation techniques for generating high-resolution, on-site rainfall data under climate model projections and hydrological simulations for evaluating the performance of the drainage systems. The framework is able to address multiple types of uncertainties arising from climate change scenarios, model randomness and rainfall design types and is straightforward to apply. A small urban catchment in the tropical region is used as the study catchment for demonstration.

Study area and data

A small urban catchment located at a tropical city is selected to demonstrate the proposed framework (Le *et al.* 2014). Figure 1 shows its general map and the layout of the existing drainage network of the study site. The site covers an area of about 36.4 ha and is characterized by urban commercial and residential areas under a tropical climate, where the average rainy days (a rainy day refers to the day with a total rainfall of 0.2 mm or more) are about 167 days in a year and the maximum 1-h rainfall depth could reach up to 147 mm (Meteorological Service Singapore 2019). The observed rainfall data used for this site include hourly time series for the baseline period from 1980 to 2010. Other observed weather data, including maximum temperature, minimum temperature and solar radiation, over the same period for the study site are obtained from the Climate Forecast System Reanalysis (NCEP 2019).

METHODS

System framework

Figure 2 shows a flowchart of the overall methodology. There are five major components in the integrated
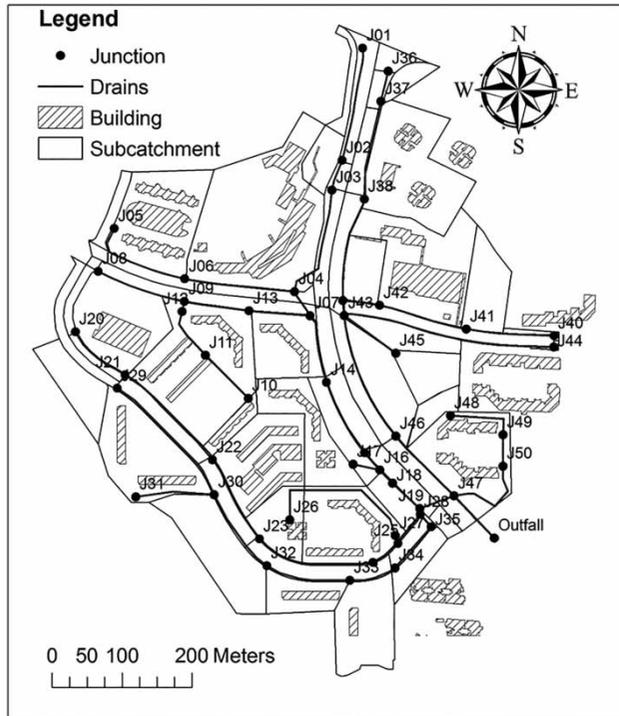
Figure 1 │ Map of land use and the drainage system for the study site.

framework, including generator setup, future scenario generation, rainfall disaggregation, rainfall design and hydrologic simulation. Firstly, a stochastic weather generator (SWG) will be used to conduct site analysis based on long-term observed weather records (i.e., temperature, precipitation
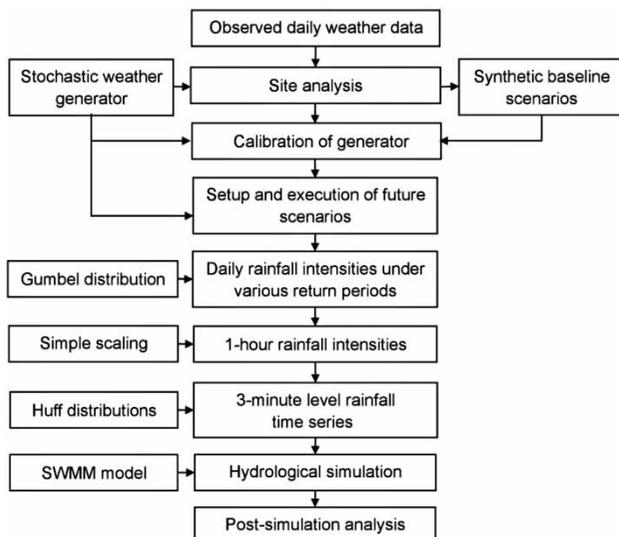

Figure 2 │ Flowchart of the overall methodology.

and solar radiation) for the study site. Secondly, future climate scenarios under various combinations (e.g., GCMs, emission scenarios and periods of prediction) are executed by the generator, and the results are used to produce daily rainfall intensities under various return periods based on the Gumbel distribution. Thirdly, the simple scaling method is applied to disaggregate rainfall from a daily timescale to an hourly one. Then, Huff distributions are adopted to generate 3-min level designed rainfalls. Finally, the designed rainfall events are used to drive hydrologic simulations to obtain runoff information. The detailed description of an individual component is given in the following sections.

Stochastic weather generator

SWGs are algorithmic models for generating the time series of climate variables, exhibiting analogous statistical properties as observed data (Semenov *et al.* 2002). They usually work for downscaling an ensemble of climate model outputs and offer probabilistic inferences about future climate impacts. The LARS-WG is one of the SWGs that has been widely used for projecting future daily weather data (including precipitation, temperature and solar radiation) at a single site (Racsko *et al.* 1991; Semenov *et al.* 1998, 2002). The latest version of this generator is LARS-WG v6, which comprises a subset of 18 GCMs with two Representative Concentration Pathway (RCP) scenarios (Semenov & Stratonovitch 2015). The two RCPs (i.e., RCP 4.5 and RCP 8.5) are categorized from the Intergovernmental Panel on Climate Change Assessment Report V (IPCC 2014). For a more detailed introduction of the LARS-WG, readers are referred to Semenov & Stratonovitch (2015).

Gumbel distribution

In hydrology, the Gumbel distribution (Gumbel 2012; Cheng *et al.* 2014) is popularly used to analyse variables such as monthly and annual maximum values of daily rainfall. When adopting the Gumbel distribution for calculating daily rainfall intensities under various return periods, the input is a vector based on the statistical analysis of the output of SWGs, and the values of the vector represent the annual maximum daily rainfall depth for a specific length of years (e.g., 100 years of record will contribute to

a vector with 100 values). Then, a bar plot is created accordingly, and a Gumbel distribution curve is fitted on the plot. Key parameters of the fitted curve include μ (location) and β (scale). In hydrology, given a return period T, the exceedance probability (P) is the reciprocal of T. Thus, in the quantile function (inverse cumulative distribution function (CDF)), the variable (y) is calculated as follows:

$$y = 1 - P = 1 - 1/T \tag{1}$$

According to the quantile function of the Gumbel distribution, the corresponding rainfall depth ($Q(y)$) is given by the following equation (Gumbel 1941):

$$Q(y) = \mu - \beta \ln(-\ln(y)) \tag{2}$$

Therefore, by adopting the Gumbel distribution, we can specify a series of return periods and obtain the corresponding maximum daily rainfall intensities.

Simple scaling method

A simple scaling method has been proved as a simple yet reliable disaggregation method (Bara *et al.* 2010; Herath *et al.* 2016; Rodríguez *et al.* 2017) since the scaling hypothesis has been verified by Menabde *et al.* (1999). The hypothesis points out that it was widely observed that the probability distributions of the annual maximum daily rainfall intensity at various durations exhibit scale invariance behaviour (Menabde *et al.* 1999). Such a behaviour could be described by a power function as follows (Bara *et al.* 2010; Rodríguez *et al.* 2017):

$$I_t^q = \lambda^{K(q)} I_{t=24\,\text{h}}^q \tag{3}$$

$$1/48 \le \lambda = t/24\,\text{h} \le 1 \tag{4}$$

where I_t and $I_{t=24\,\text{h}}$ are annual maximum rainfall intensities with a duration of t and 24 h, respectively, q is the moments of order for I_t and $I_{t=24\,\text{h}}$, $K(q)$ is a scale function of q and λ is the scale parameter of rainfall durations. If the process is assumed to be a simple scale, the scaling function $K(q)$ in Equation (3) becomes a linear function:

$$K(q) = \alpha q \tag{5}$$

where α is a scaling factor. Let $I(t,T)$ and $I(24,T)$ denote the extreme rainfall intensities with the duration of t and 24 h, respectively, where T is the return period. Based on Equations (3)–(5), the following equation can be obtained as follows:

$$I(t, T) = I(24, T) \cdot (t/24)^{\alpha} \tag{6}$$

where the scaling factor α and the relationship between $I(t,T)$ and $I(24,T)$ for a region could be derived by analysing the baseline rainfall dataset. Once the relationship is established, it could be used to disaggregate future extreme rainfall from daily timescale to hourly one.

Huff storm distributions

Knowledge of the temporal distribution of rainfall storms is of vital importance in dealing with hydrologic problems, such as the design of the urban drainage system (Huff 1967). The 1-h rainfall remains relatively coarse in a temporal resolution and is unable to describe accurately the rainfall–runoff process at the fine scales of urban drainage systems. Referring to the related previous studies, Le *et al.* (2014) chose one type of Huff storm distribution (Huff 1967) to develop design rainfall from IDF curves; Yu *et al.* (2017) considered all four types of Huff distributions for addressing uncertainty arising from the selection of different types of Huff design and further explored the impact of the temporal distribution of extreme storms on the hydraulic performance. Recently, Jun *et al.* (2018) divided historical rainstorm events in Singapore into four quartile types based on Huff's method and indicated that four types are all possible, but type II was relatively more dominant. Therefore, in this study, Huff storm distributions are adopted in the form of tabular data (Huff 1990). Based on the time interval of 5% of the total rainfall duration, 3-min level hyetographs from 1-h rainfall are derived with all four types of rainfall patterns being considered.

Establishment of the hydrological model

An urban hydrological model is normally utilized to demonstrate the hydraulic or hydrologic relations in an urban

drainage system. The US EPA Storm Water Management Model (SWMM) is a dynamic programme for linking rainfall to runoff in urban drainage networks, while tracking the water quality of runoff generated within each sub-watershed (Aad et al. 2009). It has been used worldwide for helping the design and management of urban drainage systems. The SWMM model is a complex ensemble consisting of several hydraulic–hydrological modules (e.g., subcatchments, aquifers, conduits and junctions). More technical details of the SWMM can be found in Rossman (2009).

RESULTS

Prediction by the SWG and the Gumbel distribution

LARS-WG v6 is adopted to synthesize the baseline climate condition and simulate future climate scenarios. Other alternative weather generators include the SDSM (Wilby et al. 2002) and the Downscaling-Disaggregation Weather GENerator (DD-WGEN) (Mezghani & Hingray 2009). The observed weather data are arranged into daily time series, serving as benchmark data to the LARS-WG for a calibration purpose. It is important to have a good fit of a specific distribution to historical data before we use it for synthetic data. Then, the Gumbel distribution is fitted on the historical annual maximum daily rainfall record, and the result is shown in Figure 3. The coefficient of determination (R^2) is 0.861, which shows a decent performance of the Gumbel distribution. Afterwards, synthetic baseline scenarios are generated by the LARS-WG under different

Figure 3 │ Gumbel distribution fits on the annual maximum daily rainfalls of the baseline dataset.

random seeds which are linked to the stochastic component of the generator. There are two steps of the calibration. Firstly, in the process of the site analysis, basic statistics from the generated test file are carefully checked, such as p-values and the correlation coefficient between synthetic and baseline datasets in the 'RAIN daily maxima' section. It should be noted that the selection of the section for a check is subject to the purpose of the study. We choose the 'RAIN daily maxima' section, as the intended output of the generator will be daily rainfall intensities. If these results are not satisfactory, the site analysis would need to be redone until the criteria are satisfied. Secondly, the matrix of the extreme value feature (i.e., synthetic and baseline daily rainfall intensities over various return periods) should be calculated to further identify the best random seed for calibrating the generator (Semenov et al. 2002). For each synthetic scenario, the Gumbel distribution is adopted to generate daily rainfall intensities under various return periods. In this study, we set the threshold of p-values at 0.95 and the correlation coefficient between synthetic and baseline daily maximum rain datasets (i.e., the median, 95 percentile and maximum values in 12 months of a year) all at a threshold of 0.8. The results indicate that the best seed could achieve an average relative error (defined as the sum of percentage differences between the corresponding elements of two sets divided by the common length of these two sets) around 0.36% based on the comparison of the synthetic daily rainfall intensities and the baseline intensities over various return periods.

In this study, five GCMs, namely MIROC5, EC-EARTH, HadGEM2-ES, GFDL-CM3 and MPI-ESM-MR, under a rising radiative forcing pathway of emission (i.e., RCP 8.5) (Riahi et al. 2011) are adopted in the LARS-WG to estimate changes in the future climate for the time periods of 2061–2080. Detailed information of the adopted GCMs are provided in Supplementary Table S1. The record length of each generated climate scenario is set to be 100 years. These climate scenarios are also fitted into the Gumbel distribution, and the rainfall intensities are predicted by fitted curves and Equations (1) and (2) under various return periods. Figure 4 shows the prediction results, indicating that four out of five GCMs suggest higher rainfall intensities than the baseline scenario. HadGEM2-ES suggests a decrease in the intensity ranging from −2.9 ($T = 5$ years) to
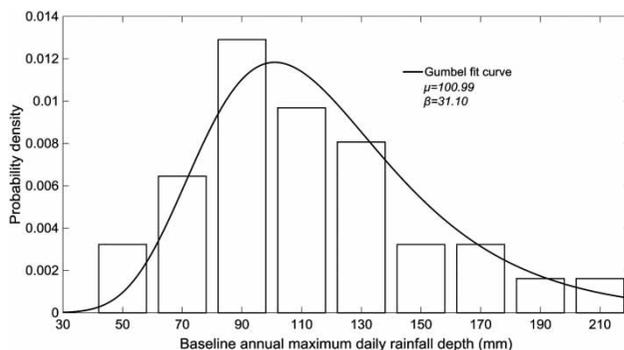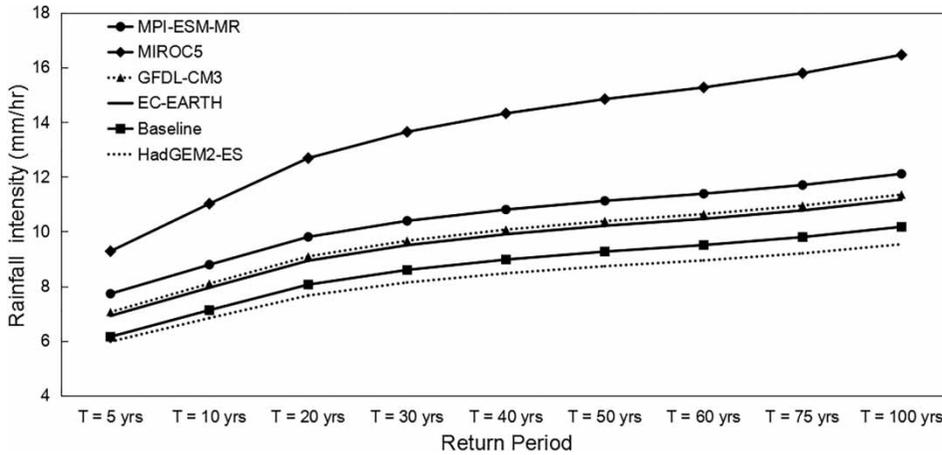
Figure 4 | Predictions of future daily rainfall intensities (i.e., $I_{t=24\,h}$) under various return periods from different GCMs under RCP 8.5 and the baseline scenario.

-6.3% ($T = 100$ years) under various return periods, and it is also found that a longer return period would lead to a larger decrease.

Disaggregation by simple scaling

The series of I_t, which denote the annual maximum mean rainfall over the time duration t (i.e., 1, 2, 3, 4, 5, 6, 8, 10, 12, 16, 20 and 24 h in this study), are derived from the baseline dataset (i.e., 1980–2010). Figure 5 shows the process of acquiring the scaling factor of simple scaling. Figure 5(a) shows the logarithmic plot of the corresponding q-order (increases from 0.5 to 3.0 at an increment of 0.5) moments I_t^q versus t. Straight lines indicate that the scale invariance is fitted by linear regressions over a temporal range from 1 to 24 h (with an average R^2 at 0.99). Similar patterns of regression have been reported previously (Bara *et al.* 2010; Rodríguez *et al.* 2014, 2017). Figure 5(b) also demonstrates a decent linear relationship between the scale function $K(q)$ (i.e., the slopes of lines in Figure 5(a)) and the order q with a scaling factor α being -0.801. Afterwards, baseline and future daily rainfall intensities (Figure 4) are disaggregated into 1-h rainfall intensities by using Equation (6) (detailed results are shown in Supplementary Table S2). MIROC5 is picked up as an example to derive IDF curves with durations from 0.5 to 3 h (see Figure 6).

Validating the results of simple scaling by the baseline dataset is essential for further design or disaggregation of rainfall. The validation procedure involves several steps.

Firstly, the series of annual maximum 1-h rainfall is extracted from the baseline dataset, and the corresponding CDF curve is generated. Secondly, the GEV distribution is
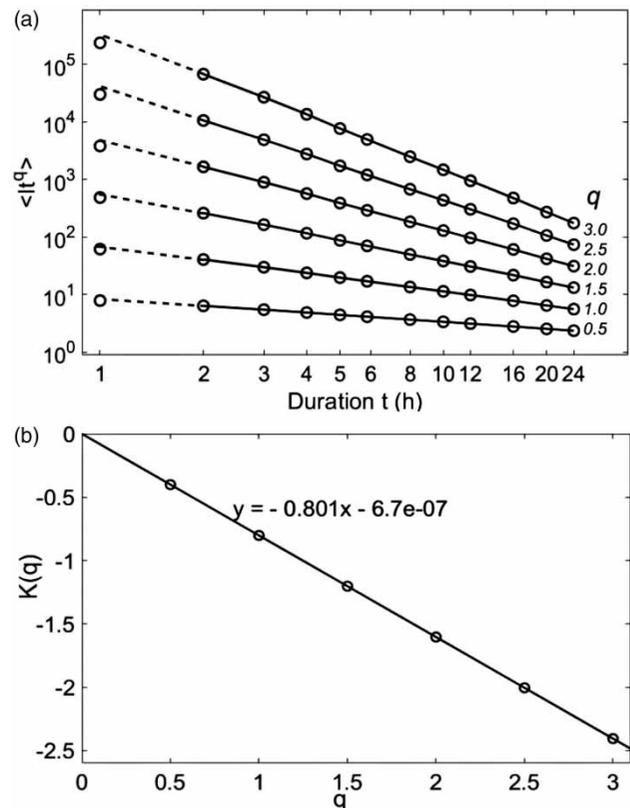

Figure 5 | (a) A logarithmic plot of statistical q-moments of the rainfall intensity (in mm/h) versus duration t (from 1 to 24 h) and (b) linear relationship between the scale function $K(q)$ and the order q of the moments in the scaling range.
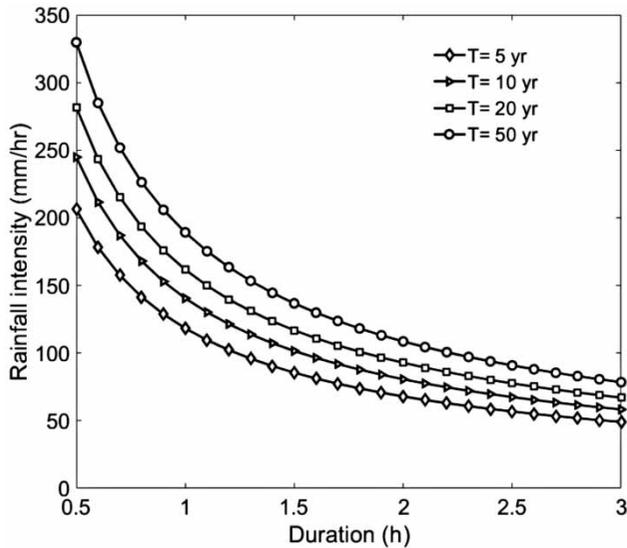
Figure 6 | IDF curves derived from the output of MIROC5 by using the simple scaling method.

used to fit the CDF curve, as it is found to be able to achieve the best fit among various types of distributions. The detailed results of GEV fitting are given in the Supplementary Figure S1. Thirdly, according to the formulation of the fitted GEV distribution, the 1-h rainfall intensities under various return periods are calculated. As shown in Table 1, by comparing the results of rainfall intensities between simple scaling and GEV fitting, it is found that the relative errors for all the return periods are lower than 10%. The performance of simple scaling is considered as acceptable for our study purpose.

Rainfall design by the Huff distribution

Huff distributions are adopted to design rainfall at the temporal resolution of minutes. The suitability of the Huff

Table 1 | Comparison between the results of rainfall intensities based on simple scaling and GEV fitting of the baseline

Source	Return period T (year)			
	5	10	20	50
GEV fitting (mm)	85.5	92.8	99.3	107.0
Simple scaling (mm)	78.5	90.9	102.8	118.2
Relative error (%)	8.9	2.1	−3.4	−9.5

design also needs to be verified by the baseline dataset. We have collected 1-min interval rainfall data with 1-year duration (i.e., July 2010 to June 2011) from the study area. The threshold of the rainfall depth is set to 30 mm for identifying individual large storm events with durations being around 1 h (i.e., 0.5–2 h). As a result, 18 events are identified, and these events are divided into four quartile groups, depending on the location where the peak rainfall intensity occurs. It is shown that the number of events categorized into quartile groups I, II, III and IV are 4, 8, 5 and 1, respectively. For a clear view of rainfall patterns, T/T_d (i.e., the ratio of cumulative time T over total rainfall duration T_d) versus P/P_d (i.e., the ratio of cumulative rainfall depth P over total rainfall depth P_d) is plotted for each identified event and four types of Huff distributions. It is found that the shapes of actual rainfall events are much more complex than the idealized Huff curves, and many real events are even multimodal instead of the Huff curves' sole peak point. However, a general qualitative comparison indicates that each quartile group shares some similarities with the corresponding type of Huff distribution regarding the overall shape and the location of peak point. More details can be found in Supplementary Figures S2 and S3.

Hydrologic simulation and post-simulation analysis

An urban hydrological model based on the SWMM is established for the study site. The model mainly consists of 55 subcatchments, 50 junctions, 50 conduits and 1 outfall. To improve the reliability of the model before carrying out any simulations, it is important to calibrate the model by comparing the model outputs with the observed record. According to Le *et al.* (2014), the SWMM was calibrated and verified by measured water-level data over a number of rainfall events at two downstream gauging stations. As an example, the measured hydrograph of one rainfall event occurring in 2012 showed that the SWMM produced very close flows to the observed data (especially the peak flows), with the R^2 value being above 0.90 (detailed information can be referred in Supplementary Figure S4). It should be noted that rainfall is the most important weather information for calibrating and driving the hydrological model in this study. Other weather variables like

temperature and radiation are considered negligible in the calibration due to short-term simulations.

Figure 7 summarizes various SWMM outputs driven by the designed 3-min level rainfall time series under Huff type I distribution. Figure 7(a) and 7(b) denote the maximum flow and time to peak at the outfall, respectively; Figure 7(c) and 7(d) show the total outflow from the system (i.e., the sum of the discharge volume at the outfall and system flood volume) and the system flood volume, respectively. It appears that the maximum flow (Figure 7(a)), system outflow (Figure 7(c)) and system flood volume (Figure 7(d)) are all dependent on the rainfall intensity; however, among these outputs, the degrees of sensitivity vary notably. The maximum flow at the outfall is relatively insensitive to the rainfall intensity, especially for intensive rainfall events: for $T = 50$ years, the 1-h rainfall ranges from 111.3 mm (HadGEM2-ES) to 189.2 mm (MIRCO5, 1.70 times of HadGEM2-ES), and this would lead to the maximum flow ranging from 26.6 (HadGEM2-ES) to 28.7 m^3/s (MIROC5, 1.08 times of HadGEM2-ES), whereas both the system outflow and system flooding are highly sensitive to rainfall, and the volume of flash flood could reach up to 18,789 m^3 (MIROC5, $T = 50$ years). In comparison, the baseline scenarios ($I_t = 118.2$ mm/h, $T = 50$ years) would lead to

a flood volume of 4,727 m^3. The time to peak under most scenarios fluctuates within the range of 13–15 min, implying low sensitivity of this output towards the rainfall intensity.

Based on the SWMM settings, if the small fraction of the loss of rainfall (e.g., evaporation and infiltration) is ignored, the runoff would all be drained to the drainage system. Hence, they could either be the discharge leaving the system from the outfall or the flooding coming out of junctions and getting lost from the system. Therefore, the system outflow (i.e., discharge plus flooding; Figure 7(c)) could be directly compared with the input rainfall depth, and the system flooding (Figure 7(d)) reflects the deficiency of the drainage capacity towards the rainfall input. From Figure 7(d), under Huff type I distribution, the existing drainage system in this case study could only accommodate the rainfall up to a 10-year return period under the current climate or 'weak' GCM like HadGEM2-ES, but fail on the rainfall under 'strong' GCM like MIROC5. Generally speaking, when the amount of rainfall increases above a certain threshold (e.g., 90 mm/h), the conveyance capacity of the drainage network would be exhausted and a further increase in rainfall would only result in more flooding, while the maximum flow at the outfall (Figure 7(a)) remains somewhat stable.
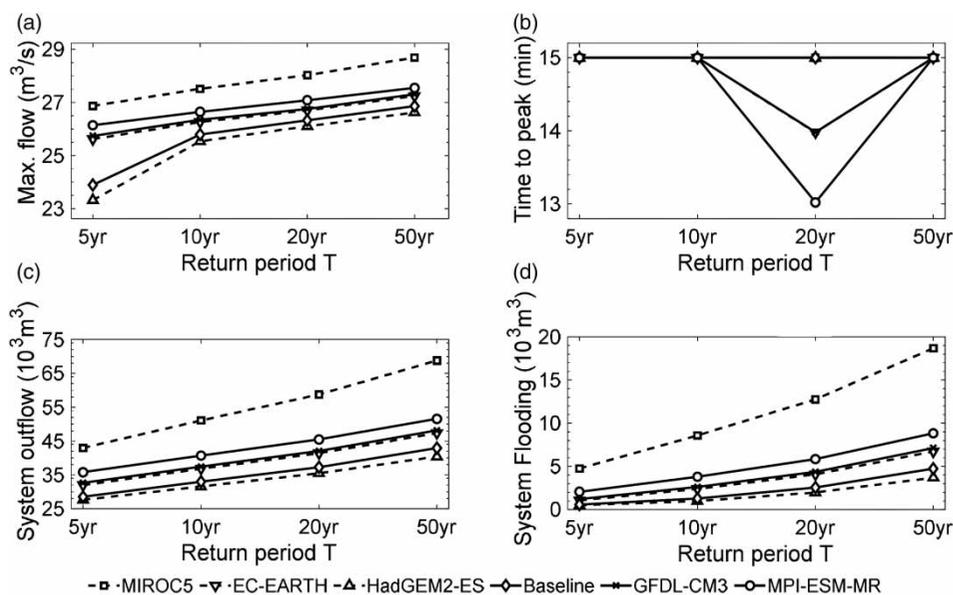

Figure 7 │ SWMM output under Huff type I distribution: (a) maximum flow at the outfall, (b) time to peak on the outfall, (c) total outflow from the system and (d) system flooding caused by extreme rainfall events from different GCM outputs and the baseline condition.

The comparison of model results among rainfall events with different types of Huff distributions is useful to further understand the temporal distribution of extreme storms on the urban drainage system. Figure 8 shows the outfall loading, system outflow and system flood volume driven by GFDL-CM3 (which suggests a moderate rainfall intensity) under different types of Huff distributions and return periods. From Figure 8, rainfall with Huff type IV distribution would lead to the highest maximum flow at the outfall (up to 27.9 m^3/s) and the worst flood condition (up to a total flood volume of 8,262 m^3), whereas rainfall with Huff type II would give the most optimistic output. From Figure 8(a) and 8(d), under a fixed rainfall intensity (i.e., the same GCM and return period), a larger maximum flow at the outfall may indicate a more severe flooding, as some patterns of rainfall distribution could result in a concentrated runoff over a short time period that challenges the drainage capacity. The system outflow (Figure 8(c)) is directly influenced by the input rainfall depth. For instance, the rainfall depth is 90.0 mm under $T = 5$ years, which will result in a volume of 327.4 (unit in 10^3 m^3, hereinafter the same) within the area of the study catchment. This volume is very close to the system outflows (ranging from 325.8 to 326.1×10^3 m^3) under four Huff types. The maximum hydrograph value (Figure 8(a)) is more sensitive to Huff types

from rainfalls with a lower intensity. For instance, under $T = 5$ years, the peak values are 19.4, 25.2, 25.7 and 26.6 m^3/s for types II, III, I and IV, respectively (i.e., the ratio of the peak value is 1.00:1.30:1.32:1.37 for types II:III:I:IV, respectively); whereas under $T = 50$ years, the corresponding ratio would be 1.00:1.05:1.06:1.08. The time to peak (Figure 8(b)) is mainly influenced by the type of Huff distribution, as it does not vary significantly over different return periods. The magnitude of flooding (Figure 8(d)) is the most sensitive SWMM output to the types of Huff distributions. Taking T of 50 years as an example, the volumes of system flood are 2,451; 5,550; 7,136 and 8,262 m^3 (with ratios at 1.00:2.26:2.91:3.37) under type II, III, I and IV design rainfall patterns, respectively. This indicates the impact of the temporal distribution of extreme storms on the hydraulic performance of the drainage system. Under $T = 50$ years, Figure 9 shows the hyetograph and hydrograph at the outfall for rainfalls with four types of Huff distributions. Figure 9(a) shows a sharp increase of runoff at about 15 min, and the peak runoff stabilizes at around 27 m^3/s for about 10 min; Figure 9(b) demonstrates that the maximum flow of 25.9 m^3/s would occur after the peak of rainfall at about 24 min; Figure 9(c) indicates a fluctuation of runoff in the first half hour before it reaches its peak at about 41 min and Figure 9(d) illustrates that the
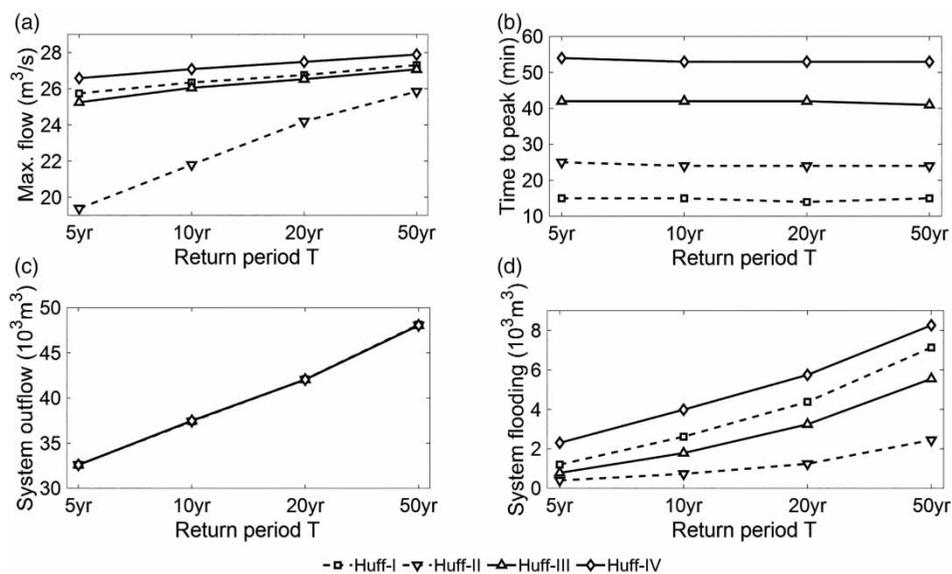

Figure 8 | SWMM output based on GCM model GFDL-CM3: (a) maximum flow at the outfall, (b) time to peak at the outfall, (c) total outflow from the system and (d) system flooding caused by extreme rainfall events from different Huff types of distribution and return periods.
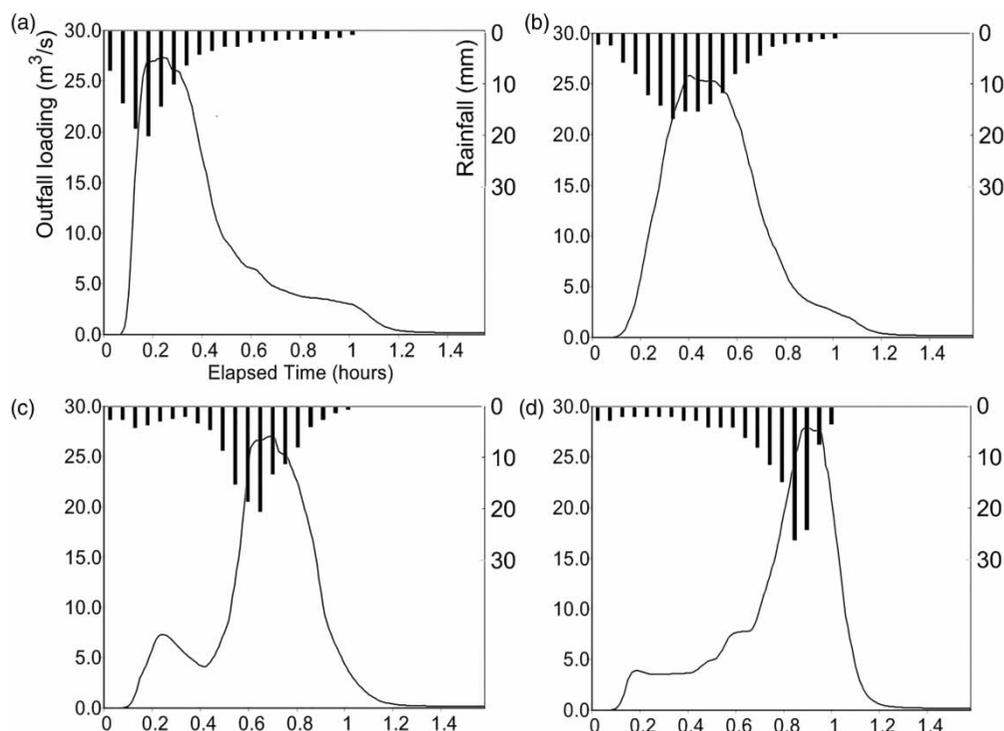
Figure 9 | Hyetograph and hydrograph at the outfall based on the GFDL-CM3 model for rainfall events with a 50-year return period and Huff distribution: (a) type I, (b) type II, (c) type III and (d) type IV.

highest peak flow of 27.9 m³/s would occur at about 51 min. The change of Huff types could also have a great effect on the spatial distribution of flooding, and the detailed information is provided in Supplementary Figure S5.

DISCUSSION

This study attempts to integrate various techniques into a holistic framework for assessing climate change impact on extreme rainfall and the urban drainage system. These techniques involve the SWG, the Gumbel distribution, the simple scaling method, the Huff distribution and urban drainage modelling. The outputs of five GCMs are disaggregated to 1-h rainfall and further converted to 3-min level designed rainfall, which are used to drive an urban drainage model. Statistical validations of each component of the framework are also provided to form a rigorous framework. It is revealed that under the emission scenario of RCP 8.5, the selection of different GCMs has a remarkable impact

on the future daily rainfall intensities under various return periods when compared to the baseline condition (Figure 4). Both GCMs and the type of Huff distributions play important roles in the outfall runoff and flooding condition of the drainage system (Figures 7–9).

The proposed framework is proved to have a number of advantages. Firstly, the proposed framework is simple to use, rigorous and comprehensive in the climate change impact assessment and urban drainage studies. By adopting a simple yet efficient disaggregation method (i.e., simple scaling), it allows the estimation of future design rainfall at hourly resolution with selected return periods by using only a power-law relationship along with rainfall information from GCMs. By tracking outputs from the hydrologic model, the impact of climate change could directly project to the drainage flow which is particularly useful for evaluating the performance and design of the drainage system under various conditions. Secondly, the proposed framework addresses multiple types of uncertainties. The uncertainty arising from the selection of climate

change scenarios is addressed by incorporating five representative GCMs for future rainfall projections as the first step. The model randomness of the weather generator is addressed and restrained by a two-step calibration procedure to make sure that the generator adopts appropriate parameters (e.g., random seed) and produces feasible outputs. Also, four types of Huff distributions are considered for rainfall design. The capability of addressing these uncertainties could help evaluate holistic impacts from future climate change, downscaling and disaggregation in comparison to the baseline scenario obtained from the historical record. Obviously, more scenarios could be easily added if a more comprehensive evaluation is of interest.

To implement the proposed framework, we also encountered some limitations. The hydrologic simulations for future climate scenarios are based on the current catchment without considering changes over time such as urban development, land-use changes and local implementation of low impact development (Willems et al. 2012). In addition, the study catchment adopted in this study was relatively small. But, we believe that this size is sufficient for applying single-site rainfall disaggregation. However, if a large size catchment is considered, multi-site correlation issues may have to be addressed using more sophisticated weather generators. For instance, Mezghani & Hingray (2009) presented a weather generator developed for the multi-site generation of hourly precipitation time series over complex terrain, and the generator could reproduce spatial and temporal correlation between weather variables (e.g., precipitation) at different scales. Lastly, under the same return period T, the maximum rainfall intensity at one point is always larger than the maximum areal average intensities (Fowler et al. 2005). Thus, for further application at larger scales (e.g., a city scale), the concept of areal reduction factors (Allen & DeGaetano 2005) could be adopted as a bridge to relate the maximum areal average rainfall rate to the maximum rate estimated at a point (e.g., observations from rain gauges and downscaled results of simple scaling).

CONCLUSIONS

An integrated framework was proposed for supporting the climate change impact assessment on extreme rainfall and urban drainage. The framework adopts the SWG for future climate scenario acquisition, the simple scaling method and Huff distributions for rainfall disaggregation and design, and the hydrologic model for the rainfall–runoff simulation. An urban catchment located in the tropical rainforest climate region was selected for demonstrating the detailed procedures, applicability and rigour of methodology. The results showed that the selection of different GCMs has a noticeable impact on the future daily rainfall intensities. Meanwhile, the temporal distribution of rainfall plays important roles in the outfall runoffs and system flooding. The simple scaling method is proved to be a good alternative for tackling daily rainfall disaggregation. Conventional methods may lack the capability of coalescing various modules (e.g., downscaling, disaggregation and hydrological simulation) into a rigorous framework while considering uncertainties arising from different sources (e.g., the selection of GCMs and rainfall patterns). The proposed framework is easy to implement and a promising alternative to conventional methods for evaluating the performance and design of the drainage system under various types of uncertainties. The overall methodology is general, and the adopted models/tools are mostly open source and easily accessible. Therefore, it is believed that this work could be generalized to many urban areas around the world to address the climate change impact on the drainage flow and urban flooding problems.

SUPPLEMENTARY MATERIAL

The Supplementary Material for this paper is available online at https://dx.doi.org/10.2166/nh.2019.233.

REFERENCES

Aad, M. P. A., Suidan, M. T. & Shuster, W. D. 2009 Modeling techniques of best management practices: rain barrels and rain gardens using EPA SWMM-5. *Journal of Hydrologic Engineering* **15** (6), 434–443. https://doi.org/10.1061/(ASCE)HE.1943-5584.0000136.

Alamdari, N., Sample, D. J., Steinberg, P., Ross, A. C. & Easton, Z. M. 2017 Assessing the effects of climate change on water quantity and quality in an urban watershed using a calibrated stormwater model. *Water* **9** (7), 464. https://doi.org/10.3390/w9070464.

Allen, R. J. & DeGaetano, A. T. 2005 Areal reduction factors for two eastern United States regions with high rain-gauge density. *Journal of Hydrologic Engineering* **10** (4), 327–335. https://doi.org/10.3390/w9070464.

Bara, M., Gaál, L., Kohnová, S., Szolgay, J. & Lavčová, K. 2010 On the use of the simple scaling of heavy rainfall in a regional estimation of IDF curves in Slovakia. *Journal of Hydrology and Hydromechanics* **58** (1), 49–63. https://doi.org/10.2478/v10098-010-0006-0.

Bi, E. G., Gachon, P., Vrac, M. & Monette, F. 2017 Which downscaled rainfall data for climate change impact studies in urban areas? Review of current approaches and trends. *Theoretical and Applied Climatology* **127** (3–4), 685–699. https://doi.org/10.1007/s00704-015-1656-y.

Cheng, L., AghaKouchak, A., Gilleland, E. & Katz, R. W. 2014 Non-stationary extreme value analysis in a changing climate. *Climatic Change* **127** (2), 353–369. https://doi.org/10.1007/s10584-014-1254-5.

Fischer, E. M. & Knutti, R. 2016 Observed heavy precipitation increase confirms theory and early models. *Nature Climate Change* **6** (11), 986. https://doi.org/10.1038/nclimate3110.

Fong, M. 2012 *The Weather and Climate of Singapore*. Meteorological Service Singapore, Singapore, 228 pp.

Fowler, H. J., Ekström, M., Kilsby, C. G. & Jones, P. D. 2005 New estimates of future changes in extreme rainfall across the UK using regional climate model integrations. 1. Assessment of control climate. *Journal of Hydrology* **300** (1–4), 212–233. https://doi.org/10.1016/j.jhydrol.2004.06.017.

Gumbel, E. J. 1941 The return period of flood flows. *The Annals of Mathematical Statistics* **12**, 163–190.

Gumbel, E. J. 2012 *Statistics of Extremes*. Columbia University Press, New York, NY, USA.

Herath, S. M., Sarukkalige, P. R. & Nguyen, V. T. V. 2016 A spatial temporal downscaling approach to development of IDF relations for Perth airport region in the context of climate change. *Hydrological Sciences Journal* **61** (11), 2061–2070. https://doi.org/10.1080/02626667.2015.1083103.

Huff, F. A. 1967 Time distribution of rainfall in heavy storms. *Water Resource Research* **3** (4), 1007–1019. https://doi.org/10.1029/WR003i004p01007.

Huff, F. A. 1990 *Time Distributions of Heavy Rainstorms in Illinois*. Illinois State Water Survey, Champaign, Circular 173, 1990. Available from: https://www.isws.illinois.edu/pubdoc/C/ISWSC-173.pdf (accessed 1 November 2019).

Intergovernmental Panel on Climate Change (IPCC) 2007 *Climate Change 2007: Synthesis Report. Contribution of Working Groups I, II and III to the Fourth Assessment Report of the Intergovernmental Panel on Climate Change* (Core Writing Team, R. K. Pachauri & A. Reisinger, eds). IPCC, Geneva, Switzerland.

Intergovernmental Panel on Climate Change (IPCC) 2014 *Climate Change 2014: Synthesis Report. Contribution of Working Groups I, II and III to the Fifth Assessment Report of the Intergovernmental Panel on Climate Change* (R. K. Pachauri & L. A. Meyer, eds). IPCC, Geneva, Switzerland.

Jun, C., Qin, X. S. & Lu, W. 2018 Temporal pattern analysis of rainstorm events for supporting rainfall design in a tropical city. In: *New Trends in Urban Drainage Modelling (UDM2018, Palermo, Italy, 23–26 September 2018). Green Energy and Technology* (G. Mannina, ed.). Springer, Cham, pp. 380–384. https://doi.org/10.1007/978-3-319-99867-1_64.

Koutsoyiannis, D. & Onof, C. 2001 Rainfall disaggregation using adjusting procedures on a Poisson cluster model. *Journal of Hydrology* **246** (1–4), 109–122. https://doi.org/10.1016/S0022-1694(01)00363-8.

Kristvik, E., Kleiven, G. H., Lohne, J. & Muthanna, T. M. 2018 Assessing the robustness of raingardens under climate change using SDSM and temporal downscaling. *Water Science and Technology* **77** (6), 1640–1650. https://doi.org/10.2166/wst.2018.043.

Langeveld, J. G., Schilperoort, R. P. S. & Weijers, S. R. 2013 Climate change and urban wastewater infrastructure: there is more to explore. *Journal of Hydrology* **476**, 112–119. https://doi.org/10.1016/j.jhydrol.2012.10.021.

Le, Q. T., Lu, Y., Qin, X. S. & Min, R. 2014 Assessing climate change on urban drainage flow: a case study of Singapore. In: *Proceedings of 13th International Conference on Urban Drainage*. IWA, IAHR, London, pp. 1–9.

Lu, Y. & Qin, X. S. 2014 Multisite rainfall downscaling and disaggregation in a tropical urban area. *Journal of Hydrology* **509**, 55–65. https://doi.org/10.1016/j.jhydrol.2013.11.027.

Lu, W., Qin, X. S. & Jun, C. 2019 A parsimonious framework of evaluating WSUD features in urban flood mitigation. *Journal of Environmental Informatics* **33** (1). https://doi.org/10.3808/jei.201700373.

Menabde, M., Seed, A. & Pegram, G. 1999 A simple scaling model for extreme rainfall. *Water Resource Research* **35** (1), 335–339. https://doi.org/10.1029/1998WR900012.

Meteorological Service Singapore 2019 *Climate of Singapore*. Available from: http://www.weather.gov.sg/climate/ (accessed 14 May 2019).

Mezghani, A. & Hingray, B. 2009 A combined downscaling-disaggregation weather generator for stochastic generation of multisite hourly weather variables over complex terrain: development and multi-scale validation for the Upper Rhone River basin. *Journal of Hydrology* **377** (3–4), 245–260. https://doi.org/10.1016/j.jhydrol.2009.08.033.

National Centers for Environmental Prediction (NCEP) 2019 *Global Weather Data for SWAT*. Available from: https://globalweather.tamu.edu/ (accessed 14 May 2019).

Neumann, J. E., Price, J., Chinowsky, P., Wright, L., Ludwig, L., Streeter, R., Jones, R., Smith, J. B., Perkins, W., Jantarasami, L. & Martinich, J. 2015 Climate change risks to US infrastructure: impacts on roads, bridges, coastal development, and urban drainage. *Climatic Change* **131** (1), 97–109. https://doi.org/10.1007/s10584-013-1037-4.

Olsson, J., Berggren, K., Olofsson, M. & Viklander, M. 2009 Applying climate model precipitation scenarios for urban hydrological assessment: a case study in Kalmar City, Sweden. *Atmospheric Research* **92** (3), 364–375. https://doi.org/10.1016/j.atmosres.2009.01.015.

Racsko, P., Szeidl, L. & Semenov, M. 1991 A serial approach to local stochastic weather models. *Ecological Modelling* **57**, 27–41. https://doi.org/10.1016/0304-3800(91)90053-4.

Riahi, K., Rao, S., Krey, V., Cho, C., Chirkov, V., Fischer, G., Kindermann, G., Nakicenovic, N. & Rafaj, P. 2011 RCP 8.5 – a scenario of comparatively high greenhouse gas emissions. *Climatic Change* **109** (1–2), 33. https://doi.org/10.1007/s10584-011-0149-y.

Rodríguez, R., Navarro, X., Casas, M. C., Ribalaygua, J., Russo, B., Pouget, L. & Redaño, A. 2014 Influence of climate change on IDF curves for the metropolitan area of Barcelona (Spain). *International Journal of Climatology* **34** (3), 643–654. https://doi.org/10.1002/joc.3712.

Rodríguez, R., Casas, M. C., Navarro, X. & Redaño, Á. 2017 A study of the scaling properties of rainfall in Spain and its appropriateness to generate intensity-duration-frequency curves from daily records. *International Journal of Climatology* **37** (2), 770–780. https://doi.org/10.1002/joc.4738.

Rossman, L. A. 2009 *Storm Water Management Model (SWMM) Version 5.0*. Available from: http://www.epa.gov/ednnrmrl/models/swmm (accessed 14 May 2019).

Semadeni-Davies, A., Hernebring, C., Svensson, G. & Gustafsson, L. G. 2008a The impacts of climate change and urbanisation on drainage in Helsingborg, Sweden: combined sewer system. *Journal of Hydrology* **350** (1–2), 100–113. https://doi.org/10.1016/j.jhydrol.2007.05.028.

Semadeni-Davies, A., Hernebring, C., Svensson, G. & Gustafsson, L. G. 2008b The impacts of climate change and urbanisation on drainage in Helsingborg, Sweden: combined sewer system. *Journal of Hydrology* **350** (1–2), 114–125. https://doi.org/10.1016/j.jhydrol.2007.11.006.

Semenov, M. A. & Stratonovitch, P. 2015 Adapting wheat ideotypes for climate change: accounting for uncertainties in CMIP5 climate projections. *Climate Research* **65**, 123–139. https://doi.org/10.3354/cr01297.

Semenov, M. A., Brooks, R. J., Barrow, E. M. & Richardson, C. W. 1998 Comparison of the WGEN and LARS-WG stochastic weather generators for diverse climates. *Climate Research* **10** (2), 95–107. https://doi.org/10.3354/cr010095.

Semenov, M. A., Barrow, E. M. & Lars-Wg, A. 2002 *A stochastic weather generator for use in climate impact studies*. User Man Herts, UK.

Sharma, D., Gupta, A. D. & Babel, M. S. 2007 Spatial disaggregation of bias-corrected GCM precipitation for improved hydrologic simulation: Ping River Basin, Thailand. *Hydrology and Earth System Sciences* **11** (4), 373–1390.

Shrestha, A. 2013 *Impact of Climate Change on Urban Flooding in Sukhumvit Area of Bangkok*. Doctoral Dissertation, Master's Thesis, Asian Institute of Technology, Khlong Nung, Thailand.

Shrestha, A., Chaosakul, T. A., Priyankara, D. P., Chuyen, L. H., Myat, S. S., Syne, N. K., Irvine, K. N., Koottatep, T. & Babel, M. S. 2014 Application of PCSWMM to explore possible climate change impacts on surface flooding in a peri-urban area of Pathumthani, Thailand. *Journal of Water Management Modeling*. https://doi.org/10.14796/JWMM.C377.

Shrestha, A., Babel, M. S., Weesakul, S. & Vojinovic, Z. 2017 Developing intensity–duration–frequency (IDF) curves under climate change uncertainty: the case of Bangkok, Thailand. *Water* **9** (2), 145. https://doi.org/10.3390/w9020145.

Wilby, R. L., Dawson, C. W. & Barrow, E. M. 2002 SDSM – a decisionsupport tool for the assessment of regional climate change impacts. *Environmental Modelling & Software* **17** (2), 145–157.

Willems, P. 2013 Revision of urban drainage design rules after assessment of climate change impacts on precipitation extremes at Uccle, Belgium. *Journal of Hydrology* **496**, 166–177. https://doi.org/10.1016/j.jhydrol.2013.05.037.

Willems, P., Arnbjerg-Nielsen, K., Olsson, J. & Nguyen, V. T. V. 2012 Climate change impact assessment on urban rainfall extremes and urban drainage: methods and shortcomings. *Atmospheric Research* **103**, 106–118. https://doi.org/10.1016/j.atmosres.2011.04.003.

Yu, J., Qin, X., Chiew, Y. M., Min, R. & Shen, X. 2017 Stochastic optimization model for supporting urban drainage design under complexity. *Journal of Water Resources Planning and Management* **143** (9), 05017008. https://doi.org/10.1061/(ASCE)WR.1943-5452.0000806.

Zahmatkesh, Z., Burian, S. J., Karamouz, M., Tavakol-Davani, H. & Goharian, E. 2015 Low-impact development practices to mitigate climate change effects on urban stormwater runoff: case study of New York City. *Journal of Irrigation and Drainage Engineering* **141** (1). https://doi.org/10.1061/(ASCE)IR.1943-4774.0000770.